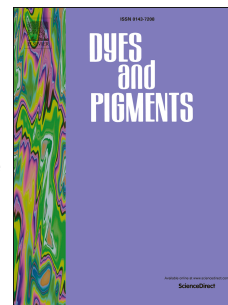# Accepted Manuscript

Structural and electronic properties of 2,2′,6,6′-tetraphenyl-dipyranylidene and its use as a hole-collecting interfacial layer in organic solar cells

M. Courté, M. Alaaeddine, V. Barth, L. Tortech, D. Fichou

1 **Structural and electronic properties of 2,2',6,6'-tetraphenyl-**

2 **dipyranylidene and its use as a hole-collecting interfacial layer in**

3 **organic solar cells**

4 M. Courté,[‡a] M. Alaaeddine,[‡b,c,d] V. Barth,[b,c,d] L. Tortech,[b,c,d] and D. Fichou [a,b,c,*]

5 *[a] School of Physical and Mathematical Sciences, Nanyang Technological University,*

6 *637371, Singapore.*

7 *[b] Sorbonne Universités, UPMC Univ Paris 06, UMR 8232, Institut Parisien de Chimie*

8 *Moléculaire, F-75005, Paris, France.*

9 *[c] CNRS, UMR 8232, Institut Parisien de Chimie Moléculaire, F-75005, Paris, France*

10 *[d] CEA Saclay, IRAMIS, NIMBE, LICSEN, F-91191 Gif-sur-Yvette, France*

11 *‡ These two authors have contributed equally to the work.*

12

13 * Corresponding author

14 E-mail address: denisfichou@ntu.edu.sg

15

16 **Abstract**

17 The accumulation of positive charges at the anodic interface considerably limits the

18 efficiency of photovoltaic solar cells based on polymer/fullerene bulk heterojunctions (BHJs).

19 Interfacial layers (IFLs) such as PEDOT:PSS improve charge injection but have no effect on

20 the unbalanced electron/hole transport across the BHJ. We report here the use of 2,2',6,6'-

21 tetraphenyl-dipyranylidene (DIPO-Ph$_4$), a planar quinoïd compound, as an efficient anodic IFL

22 in organic solar cells based on BHJs made of poly(3-hexylthiophene)/[6,6]-phenyl-C61-

23 butyric-acid-methyl-ester (P3HT:PCBM). When deposited under vacuum onto a glass

24 substrate, DIPO-Ph$_4$ thin films are constituted of densely packed and vertically aligned

25 crystalline needles. Current-sensing atomic force microscopy (CS-AFM) reveals a

26 considerable increase of the hole-carrying pathways in DIPO-Ph$_4$ thin films as compare to

27 PEDOT:PSS, thus revealing their hole transporting/electron blocking properties. Inserting a

28 10 nm thick IFL of DIPO-Ph$_4$ in combination with a 5 nm thick PEDOT:PSS between the ITO

29 electrode and the P3HT:PCBM film leads to photocurrent densities up to 11.5 mA/cm^2 under

30 AM 1.5G and conversion efficiencies up to 4.6%, that is substantially higher than PEDOT:PSS-

31 only devices.

34

2

1. Introduction

A strategy to improve the performance of organic solar cells (OSCs) consists of tailoring the interfaces between the organic active materials and the metallic electrodes. To this end interfacial layers (IFLs) are inserted between the active layer and the respective electrodes in order to reduce the energy barriers which promote charge carrier diffusion.[1-8] IFLs operate as selective charge extraction materials for either holes or electrons, while blocking the opposite charge carriers. Conducting polymer-based IFLs are commonly used to modify the ITO surface because they ensure an electrical ohmic contact and minimize the roughness. Poly(3,4-ethylenedioxythiophene):poly(styrenesulfonate) (PEDOT:PSS) is the ubiquitous hole transporting layer that is used in OSCs.[9] A thin PEDOT:PSS IFL increases the open-circuit voltage (Voc) and improves hole collection at the anodic interface between ITO and the photoactive material.

However, it is well-known that PEDOT:PSS suffers from several drawbacks. Its acidic character (pH=1-2) etches the ITO electrode and considerably shortens the long-term stability of the devices. Furthermore, PEDOT:PSS films are hygroscopic and exhibit weak electron blocking properties.[10-12] Another drawback is the weak visible light absorption of PEDOT:PSS that does not contribute to light harvesting in the devices.[13] Finally, PEDOT:PSS thin films often possess important structural and electrical inhomogeneities that are not compatible with reproducible device performances.

Therefore, alternative IFL materials have been investigated to substitute PEDOT:PSS in OSCs and other organic devices. Various organic materials have been explored as IFLs with the aim to improve charge collection, such as for example self-assembled monolayers of 4-nitrophenylthiolate[14] or halogenated propysilanes,[15] and graphene oxide.[16-18] In a previous work, we reported that 2,2',6,6'-tetraphenyldithiapyranylidene (DITPY-Ph$_4$) acts as

3

59   a hole collecting IFL when introduced in OSCs based on P3HT:PCBM.[19] Inorganic materials

60   have also been studied as hole collecting IFLs, in particular transition metal oxides such as

61   MoO3,[20-22] NiOx,[23,24] VOx, [25] copper based solutions [26,27] or

62   polyoxometalate.[28] Note that these IFLs can be used either as single layers or in

63   combination with a PEDOT:PSS layer.

64   In this work, we describe the structural and electronic properties of 2,2',6,6'-tetraphenyl-

65   dipyranylidene (DIPO-Ph$_4$, Fig. 1) and report on its use as an efficient hole-transporting IFL in

66   organic solar cells based on bulk heterojunctions BHJs made of poly(3-hexylthiophene) and

67   [6,6]-phenyl-C61-butyric-acid-methyl-ester (P3HT:PCBM). DIPO-Ph$_4$ is a large planar quinoïd

68   compound made of two pyranylidene heterocycles linked together by an exocyclic C=C

69   double bond in 4-4'positions relative to the two O-atoms. DIPO-Ph$_4$ is isoelectronic with

70   tetrathiafulvalene and behaves as a strong π-donor with various acceptors.[29] We reveal

71   here the remarkable needle-like morphology of vacuum-deposited crystalline DIPO-Ph$_4$ thin

72   films and show that it behaves as a more efficient anodic IFL in solar cells as compared to its

73   sulfur analog DITPY-Ph$_4$.
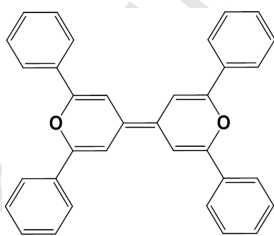
74

75

76   **Fig. 1** *Left: Chemical structure of 2,2',6,6'-tetraphenyldipyranylidene (DIPO-Ph$_4$).*

77   *Right: Deep-red shiny crystalline powder of DIPO-Ph$_4$ after purification by Soxhlet*

78   *extraction in acetonitrile.*

79

80   **2. Experimental Section**

81   *Synthesis and purification of DIPO-Ph$_4$*

82   The synthesis of DIPO-Ph$_4$ has been reported previously.[30] However, we

83   modified the synthetic protocol in order to substantially increase the yield and to

84   improve the purity of the final compound (Scheme 1). Briefly, glutaryl chloride is

85   functionalized by two phenyl groups using a Friedel-Craft acylation, and further oxidized by

86   BF$_4$.Et$_2$O into a pyrylium salt. The latter compound is then reduced by tributylphosphine

87   P(C$_4$H$_9$)$_3$ instead of zinc which is difficult to remove from the final product. The intermediate

88   ylide is finally condensed in basic medium using EtN(i-Pr)$_2$ (DIPEA) to form 2-2'-6-6'-

89   tetraphenyldipyranylidene (DIPO-Ph$_4$) in 85% yield. The raw product is a brownish

90   powder that is purified by Soxhlet extraction in acetonitrile during several days. The

91   final compound is a highly crystalline deep red powder (mp=325°C) with shiny

92   metallic reflections (Fig. 1).

93
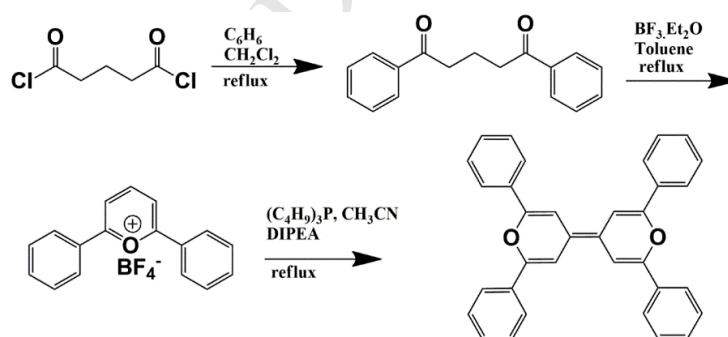
94   **Scheme. 1.** Synthetic pathway to 2,2',6,6'-tetraphenyldipyranylidene (DIPO-Ph$_4$).

95   *OPV device fabrication*

96   ITO-coated glass substrates (Sigma-Aldrich; 2.5×2.5 cm²; R=70-100 Ω/cm²) are

97   patterned by chemical etching with HCl (5 % aq.) and sonicated in successively

98   ethanol and acetone during 10 minutes. The samples are finally exposed to UV-ozone

5

99   during 10 minutes in order to remove organic impurities and improve the

100   hydrophilicity of the substrates. The crystalline DIPO-Ph$_4$ is finely divided in a mortar

101   and placed in a quartz boat. DIPO-Ph$_4$ is evaporated at a slow rate (0.1 Å/s) in a

102   thermal vacuum chamber (P$_0$~10^{-4} Pa) and the thickness is monitored by a quartz

103   microbalance (Inficon X TM/2). A 5 nm layer of PEDOT:PSS (Sigma-Aldrich; water

104   solution 1.3 % in weight) is spin-coated on top of DIPO-Ph$_4$ thin film. P3HT/PCBM bulk

105   layer is prepared by spin-coating from a solution of P3HT (Sigma-Aldrich; purity >98.5

106   %) and PCBM (Sigma-Aldrich; purity 99.5 %) dissolved in dichlorobenzene (ratio of

107   1:0.8 P3HT-PCBM) and sonicated beforehand during 10 minutes to obtain a

108   homogenous blend solution. The spin-coating conditions are adjusted to obtain 120

109   nm P3HT/PCBM thick films. The organic films undergo post-annealing at 110 °C under

110   argon during 10 min. The devices are completed by successive thermal evaporation of

111   LiF (7 Å) and Al (100 nm) through shadows mask with a diameter of 7 mm^2. The

112   reference cells were prepared by deposition of 20 nm film of PEDOT:PSS on ITO

113   followed by an annealing at 120°C under argon for 30 min. Successive layers are

114   deposited under the same conditions.

115   **3. Results and discussion**

116   The UV-visible absorption spectrum of DIPO-Ph$_4$ as recorded in

117   dichloromethane (Fig. 2) shows a structured absorption peak in the visible range

118   (λ_{max}=456 nm) with a high molar extinction coefficient 9×10^4 l/mol.cm. An absorption

119   tail of weak intensity is observed from 500 to 600 nm. Vacuum-deposited DIPO-Ph$_4$

120   thin films exhibit a much broader absorption over almost the entire visible range, with

121   an absorption edge at 640 nm and several structures assigned to absorption bands.

122   Photoluminescence spectra in solution shows a sharp peak at 606 nm. Whereas DIPO-

123   Ph_4 thin film presents two peaks at the 636 nm and 686 nm. The bandgap of DIPO-Ph_4

124   (Eg=1.9 eV) is determined from the absorption spectrum. X-ray diffraction performed

125   on DIPO-Ph_4 single crystals grown from solution reveals a parallel arrangement

126   between neighbouring planar molecules with an intermolecular distance of 3.49

127   Å.[31] Such a crystal structure is compatible with a π–stacking as well as a widening of

128   the optical absorption spectrum over the entire visible range as compared with that

129   in solution (Fig. 2b).

130   Cyclic voltammetry (Fig. S1) shows two reversible oxidation waves at respectively 0.24

131   V and 0.5 V, corresponding to the successive formation of the radical cation and

132   dication. The HOMO energy level is estimated at −4.7 eV from the first oxidation peak

133   at 0.24 V. DIPO-Ph_4 has a slightly lower oxidation potential (E_{ox}=0.24 eV) as compared

134   to that of its sulfur analog DITPY-Ph_4 (E_{ox}=0.30 eV). Therefore the highest occupied

135   molecular orbital (HOMO) of DIPO-Ph_4 intercalates adequately between ITO and P3HT

136   (E_{HOMO}=−5.0 eV) to allow hole transfer from the active layer.

137   a)   b)
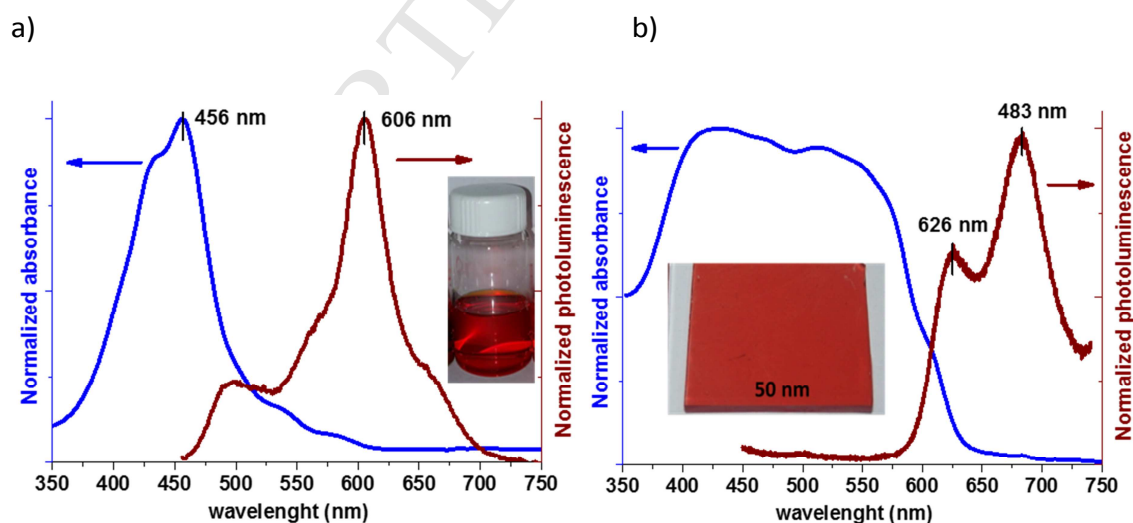

138

139   **Fig. 2** *a) Optical absorption (blue) and photoluminescence (red) spectra of DIPO-Ph$_4$ a)*

140   *in solution in dichloromethane and b) as a 50 nm thin film vacuum-deposited on*

141   *quartz. Inserts: photographs of the respective DIPO-Ph$_4$ solution and thin film.*

142   DIPO-Ph$_4$ thin films are prepared by slow vacuum-deposition (0.1 Å/s) onto

143   glass/ITO substrates. Atomic force microscopy (AFM) reveals a highly homogenous

144   surface made of monodisperse grains having an elongated needle shape (Fig. 3). A

145   distribution of the number of grains as a function of their height shows an average

146   height in the range 20-40 nm while the highest needles observed are 70 nm high. The

147   root mean square (RMS) roughness is measured at 13 nm which is much higher than

148   PEDOT:PSS film (RMS=0.9 nm). This particular nanomorphology of DIPO-Ph$_4$

149   considerably increases the contact area between the active material and the anode,

150   thus greatly enhancing hole extraction. However, in order to protect the

151   nanostructure from partial dissolution by the organic solvent during spin-coating

152   deposition of the P3HT:PCBM active layer, a 5 nm thin layer of PEDOT:PSS is spin-

153   coated (from an aqueous solution) on top of the DIPO-Ph$_4$ films. AFM images (Fig. S2)

154   confirm that the DIPO-Ph$_4$ morphology is preserved (RMS=11.3 nm). A practical

155   advantage of PEDOT:PSS film is its robustness towards organic solvents during

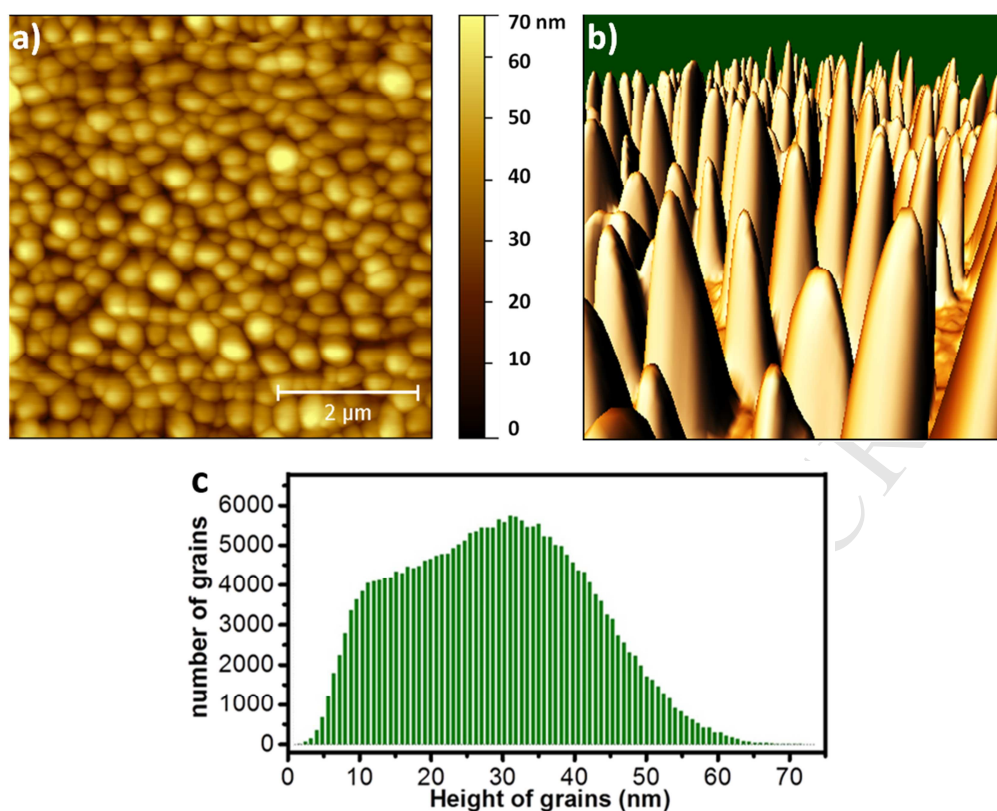156   fabrication process, making it compatible with most of organic photoactive materials.

157

158

159

Fig. 3 *(a) Tapping-mode AFM images of a 10 nm thin DIPO-Ph$_4$ film vacuum-deposited on ITO. (b) 3D lateral view of a typical AFM image of a 10 nm DIPO-Ph$_4$ thin film. (c) Distribution of the needles height in a 10 nm thin film of DIPO-Ph$_4$.*

163

Current-sensing atomic force microscopy (CS-AFM) images of DIPO-Ph$_4$ films are recorded in contact mode using either positive or negative tip voltages (Fig. 4). For a −0.3 V tip voltage the CS-AFM images exhibit high and homogeneous hole conduction with current intensities up to 10 nA. The hole conduction have preferential pathways through the grain boundaries. In comparison, CS-AFM images recorded on PEDOT:PSS films reveal insulating region and the holes are only diffused in some localized pathways which correspond to individual PEDOT domain (Fig. S3). Current mapping

9

171 recorded at +0.3 V shows a much weaker conduction of electrons as compare to
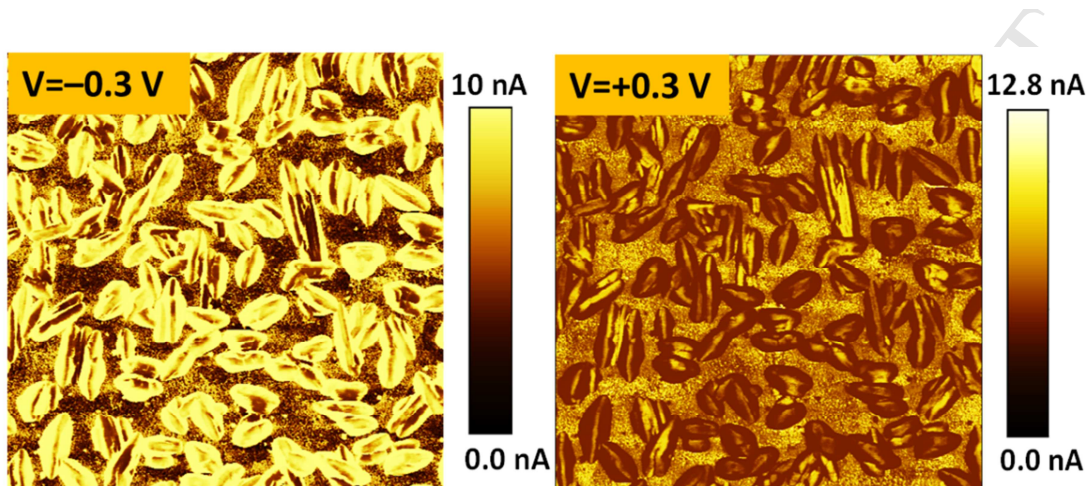
172 holes.

173

175 **Fig. 4** *CS-AFM images (5×5 μm^2) of a thin film of DIPO-Ph$_4$ (10 nm) vacuum-deposited*

176 *on an ITO/glass substrate recorded at tip voltages of −0.3 V (left) and +0.3 V (right).*

177

178   We inserted a vacuum-deposited DIPO-Ph$_4$ film (10 nm) as an anodic IFL in

179 combination with a PEDOT:PSS layer (5 nm) into P3HT:PCBM-based OSC devices

180 (Figure 5) and compared the PV performance with those of reference cells using a

181 PEDOT:PSS-only IFL. All devices have an open circuit voltage (Voc) of ≈0.6 V in

182 agreement with usual values reported for P3HT:PCBM-based devices. The short-

183 circuit current density of the reference cells is Jsc=7.6 mA.cm^{-2}, resulting in a power

184 conversion efficiency (PCE) of 2.8% (Fig. 6, blue curve). With a 10 nm thin layer of

185 DIPO-Ph$_4$, the organic solar cell exhibit higher current density. Typical devices exhibit

186 an average current density of Jsc=9.5 mA.cm^{-2} and an average PCE of 3.8% (Fig.6, red

187 curve). These characteristics correspond to a PCE increase of 35% as compare to the

188 reference cell using a PEDOT:PSS-only IFL. In the course of our experiments several

189 double-IFL devices exhibit higher current densities up to Jsc=11.5 mA.cm^{-2} with a PCE

190 of 4.6% (Fig.6, light blue curve) corresponding to a 64% increase as compare to OSCs

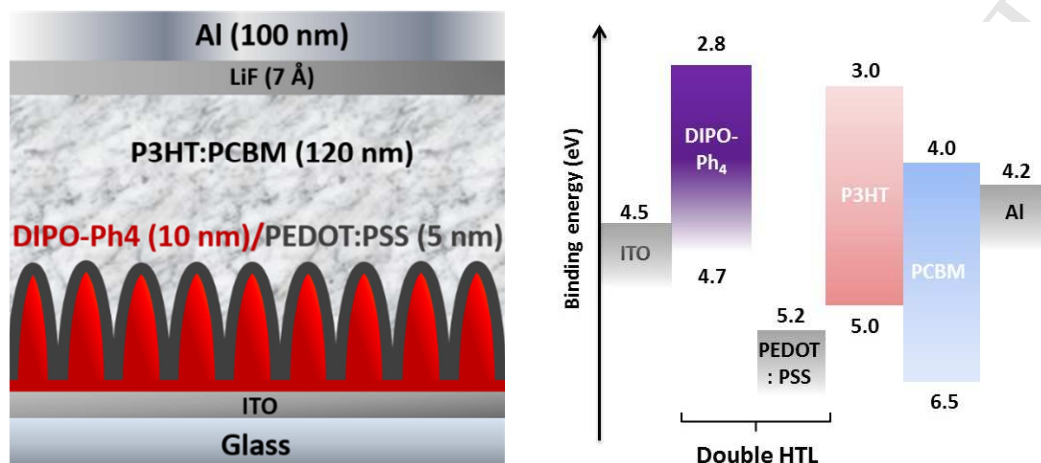191 using a PEDOT:PSS-only IFL.

193 **Fig. 5** left) Scheme of a solar cell using a double IFL: DIPO-Ph$_4$ (10 nm, red needles)

194 and PEDOT:PSS (5 nm, dark grey coating). Right) Band diagram of a solar cell using a

195 DIPO-Ph$_4$ (10 nm)/PEDOT:PSS (5 nm) double IFL.

196

197 We assign the enhanced Jsc to the high hole conduction of the DIPO-Ph$_4$ films, as

198 revealed by CS-AFM (Fig. 4). However, these higher characteristics are sample-

199 dependent due to the difficulty in controlling rigorously the nanomorphology of the

200 DIPO-Ph$_4$ films, in particular the precise height, shape and density of the crystalline

201 needles. These parameters are extremely sensitive to slight variations in the

202 deposition rate, quality of the substrate and purity of the starting materials. Indeed,

203 devices using higher DIPO-Ph$_4$ thicknesses (15 nm) show lower Voc (Fig. 6, green

204 curve) and thus a decrease in efficiency (PCE=2.5%).

205

206   a/
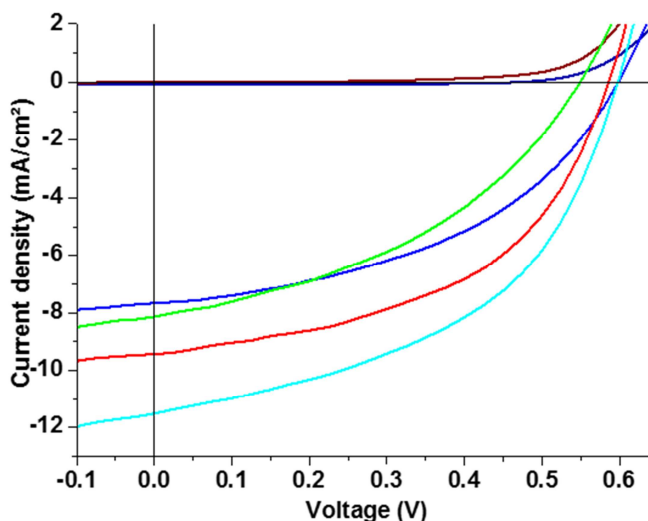
207
208   b/
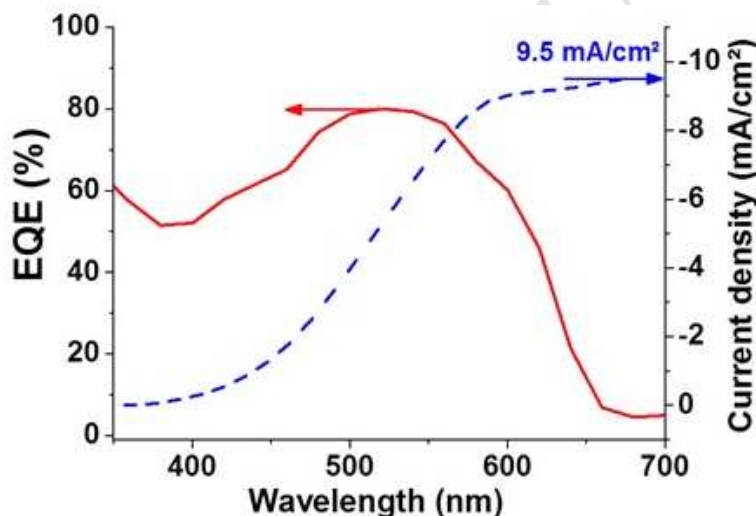
209

210   ***Fig. 6*** *(a) J-V curves measured in the dark and under white light illumination (AM 1.5G;*

211   *70 mW/cm²) of two P3HT:PCBM-based solar cells using DIPO-Ph$_4$ (10 nm; red and*

212   *cyan lines)/PEDOT:PSS (5 nm) or DIPO-Ph$_4$ (15 nm; green line) /PEDOT:PSS (5 nm) as a*

213   *double hole injecting IFL. A typical reference cell using a PEDOT:PSS-only IFL is shown*

214   *for comparison (blue line). b) EQE spectrum (red) of a PV cell using a DIPO-Ph$_4$ (10*

215   *nm)/PEDOT:PSS (5 nm) double IFL. The dashed blue line represents the integrated*

216   *current density corresponding to the red J-V curve of Fig. 6a. The PV characteristics of*

217   *our devices are summarized in Table **1**.*

218 **Table 1**

IFL		Voc (V)	Jsc (mA/cm^2)	FF	PCE (%)
PEDOT:PSS	Average values	0.60	7.6	0.44	2.8
DIPO-Ph$_4$ (10nm)/PEDOT:PSS (5nm)	Average values	0.58	9.5	0.50	3.8
	Maximum values	0.60	11.5	0.47	4.6
DIPO-Ph$_4$ (15nm)/PEDOT:PSS (5nm)	Average values	0.55	8.1	0.40	2.5

219

220 **4. Conclusions**

221   In summary, highly crystalline thin films of 2,2',6,6'-tetraphenyldipyranylidene (DIPO-Ph$_4$)

222 have been prepared by vacuum-deposition and used as hole injecting interfacial layers in

223 organic solar cells. The DIPO-Ph$_4$ thin films are made of vertically-aligned nano-needles.

224 Current-sensing atomic force microscopy (CS-AFM) reveals a considerable increase of the

225 hole-carrying pathways in DIPO-Ph$_4$ thin films as compare to PEDOT:PSS, thus revealing their

226 hole transporting/electron blocking properties. Inserting a 10 nm thick IFL of DIPO-Ph$_4$ in

227 combination with a 5 nm thick PEDOT:PSS between the ITO electrode and the P3HT:PCBM

228 film leads to photocurrent densities up to 11.5 mA/cm^2 under AM1.5G and conversion

229 efficiencies up to 4.6%, that is substantially higher than PEDOT:PSS-only devices. We are

230 currently extending this work by using DIPO-Ph$_4$ as a HTM in various types of devices,

231 including perovskite solar cells and field-effect transistors.[32] We also engineer the band

232 alignment of DIPO-Ph$_4$ by chemical design and synthesize a series of dipyranylidene analogs

233   bearing electron-donating or electron-accepting peripheral substituents around the quinoïd

234   core.

235

236   **Acknowledgements**

239

240   **Appendix A. Supplementary Data**

241   Supplementary   data   related   to   this   article   can   be   found   at

242   http://dx.doi.org/10.1016/j.dyepig

243

14

References

244

245　1　Lian J, Yuan Y, Peng E, Huang J. Interfacial layers in organic solar cells. In "*Organic*
246　　　*and Hybrid Solar Cells*", H. Huang, J. Huang (eds.), Springer International Publishing,
247　　　Switzerland, 2014.

248　2　Mazzio KA, Luscombe CK. The future of organic photovoltaics. *Chem. Soc. Rev.,* 2015*,*
249　　　**44,** 78.

250　3　Scharber MC. On the efficiency limit of conjugated Polymer:Fullerene-Based Bulk
251　　　Heterojunction Solar Cells. *Adv. Mater.*, 2016, **28**, 1994.

252　4　Duan C, Zhong C, Huang F, Cao Y. Development of Active Materials and Interface
253　　　Materials for High Performance Bulk-Heterojunction Polymer Solar Cells. In
254　　　"*Progress in High-Efficient Solution Process Organic Photovoltaic Devices*", Yang Y, Li
255　　　G (eds), Topics in Applied Physics, Vol. 130, Springer, 2015.

256　5　Cao B, He X, Fetterly CR, Olsen BC, Luber EJ, Buriak JM. Role of interfacial layers in
257　　　organic solar cells: energy level pinning versus phase segregation. *ACS Appl. Mater.*
258　　　*Interfaces*, 2016, **8**, 28.

259　6　Yin Z, Wei J, Zheng Q. Interfacial materials for organic solar cells: recent advances
260　　　and perspectives. *Adv. Sci.*, 2016, **3**, 1500362.

261　7　Park JH, Lee TW, Chin BD, Wang DH, Park OO. Roles of interlayers in efficient organic
262　　　photovoltaic devices. *Macromol. Rapid Commun.*, 2010, **31**, 2095.

263　8　Steim R, Kogler FR, Brabec CJ. Interface materials for organic solar cells. *J. Mater.*
264　　　*Chem*, 2010, **20**, 2499.

265　9　Kim W, Kim N, Kim JK, Park I, Choi YS, Wang DH et al. Polymer bulk heterojunction
266　　　solar cells with PEDOT:PSS bilayer structure as hole extraction layer. *ChemSusChem*,
267　　　2013, **6**, 1070.

268　10　Kemerink M, Timpanaro S, de Kok MM, Meulenkamp EA, Touwslager FJ. Three-
269　　　dimensional inhomogeneities in PEDOT:PSS films. *J. Phys. Chem. B*, 2004, **108**, 18820.

270　11　Girtan M, Rusu M. Role of ITO and PEDOT:PSS in stability/degradation of
271　　　polymer:fullerene bulk heterojunctions solar cells. *Sol. Energy Mater. Sol. Cells*, 2010,
272　　　**94**, 446.

273　12　Pingree LSC, MacLeod BA, Ginger DS. The changing face of PEDOT:PSS films:
274　　　substrate, bias, and processing effects on vertical charge transport. *J. Phys. Chem. C*,
275　　　2008, **112**, 7922.

276　13　Wang F, Xu Q, Tan Z, Li L, Li S, Hou X et al. Solution-processed MoO_3:PEDOT:PSS
277　　　hybrid hole transporting layer for inverted polymer solar cells *J. Mater. Chem. A,*
278　　　2014, **2**, 1318.

279　14　Hatton RA, Willis MR, Chesters MA, Rutten FJM, Briggs D. Enhanced hole injection in
280　　　organic light-emitting diodes using a SAM-derivatised ultra-thin gold anode
281　　　supported on ITO glass. *J. Mater. Chem.*, 2003, **13**, 38.

282　15　Kim JS, Park JH, Lee JH, Jo J, Kim DY, Cho K. Control of the electrode work function
283　　　and active layer morphology via surface modification of indium tin oxide for high
284　　　efficiency organic photovoltaics. *Appl. Phys. Lett.*, 2007, **91**, 112111.

285 16 Yu JC, Jang JI, Lee BR, Lee GW, Han JT, Song MH. Highly efficient polymer-based
286   optoelectronic devices using PEDOT:PSS and a GO composite layer as a hole
287   transport layer. *ACS Appl. Mater. Interfaces*, 2014, **6**, 2067.
288 17 Kishi N, Kato S, Saito T, Hayashi J, Ito D, Hayashi Y et al. Poly(3, 4-
289   ethylenedioxythiophene): Poly(styrenesulfonate)/single-wall carbon nanotube
290   composite film for the hole transport layer in polymer solar cells. *Nano*, 2011, **6**, 583.
291 18 Jeon YJ, Yun JM, Kim DY, Na SI, Kim SS. High-performance polymer solar cells with
292   moderately reduced graphene oxide as an efficient hole transporting layer. *Sol.*
293   *Energy Mater. Sol. Cells*, 2012, **105**, 96.
294 19 Berny S., Tortech L., Véber M, Fichou D. Dithiapyrannylidenes as efficient hole
295   collection interfacial layers in organic solar cells. *ACS Appl. Mater. Interfaces*, 2010,
296   **2**, 3059.
297 20 Jasieniak JJ, Seifter J, Jo J, Mates T, Heeger AJA. A solution-processed MoOx anode
298   interlayer for use within organic photovoltaic devices. *Adv. Funct. Mater.*, 2012, **22**,
299   2594.
300 21 Li B, Ren H, Yuan H, Karim A, Gong X. Room-temperature, solution-processed MoO_x
301   thin film as a hole extraction layer to substitute PEDOT/PSS in polymer solar cells.
302   *ACS Photonics*, 2014, **1**, 87.
303 22 Ohisa S, Kagami S, Pu Y-J, Chiba T, Kido J. A solution-processed heteropoly acid
304   containing MoO3 units as a hole-injection material for highly stable organic light-
305   emitting devices. *ACS Appl. Mater. Interfaces,* 2016, **8**, 20946–20954.
306 23 He S, Li S, Tan Z, Zheng H, Lin J, Hu S et al. Solution-processed nickel compound as
307   hole collection layer for efficient polymer solar cells. J. *Phys. Appl. Phys.*, 2014, **47**,
308   505101.
309 24 Manders JR, Tsang SW, Hartel MJ, Lai TH, Chen S, Am CM et al. Solution-processed
310   nickel oxide hole transport layers in high efficiency polymer photovoltaic cells *Adv.*
311   *Funct. Mater.*, 2013, **23**, 2993.
312 25 Kim J, Kim H, Kim G, Back H, Lee K. Soluble transition metal oxide/polymeric acid
313   composites for efficient hole-transport layers in polymer solar cells. *ACS Appl. Mater.*
314   *Interfaces*, 2014, **6**, 951.
315 26 Yaacobi-Gross N, Treat ND, Pattanasattayavong P, Faber H, Perumal AK, Stingelin N
316   et al. High-efficiency organic photovoltaic cells based on the solution-processable
317   hole transporting interlayer copper thiocyanate (CuSCN) as a replacement for
318   PEDOT:PSS *Adv. Energy Mater.*, 2015, **5**,1401529.
319 27 Xu Q, Wang F, Tan Z, Li L, Li S, Hou X et al. High-performance polymer solar cells with
320   solution-processed and environmentally friendly CuOx anode buffer layer. *ACS Appl.*
321   *Mater. Interfaces*, 2013, **5**, 10658.
322 28 Alaaeddine M, Zhu Q, Fichou D, Izzet G, Rault J-E, Barrett N, Tortech L. Enhancement
323   of photovoltaic efficiency by insertion of a polyoxometalate layer at the anode of an
324   organic solar cell*., Inorg. Chem. Front.*, 2014, **1**, 682.

325 29 Bolag A, Mamada M, Nishida J, Yamashita Y. Field-effect transistors based on
326   tetraphenyldipyranylidenes and the sulfur analogues. *Chem. Mater.*, 2009, **21**, 4350.
327 30 Chasseau D, Gaultier J, Hauw C. Tetraphenyldipyranylidene. *Acta Crystallogr. B*,
328   1982, **38**, 1629.
329 31 Alizon J, Gallice J, Robert H, Delplanque G, Weyl C, Fabre C et al. Nouveaux
330   complexes de transfert de charge à partir des dipyranylidenes. *Mol. Cryst. Liq. Cryst.*,
331   1976, **33**, 91.
332 32 Courté M, Surya SG, Thamankar R, Shen C, Ramgopal Rao V, Mhaisalkar SG, Fichou
333   D. A non-volatile resistive memory effect in 2,2',6,6'-tetraphenyl-dipyranylidene thin
334   films as observed in field-effect transistors and by conductive atomic force
335   microscopy. *RSC Advances*, 2017, **7**, 3336-3342.

Highlights

Structural and electronic properties of 2,2',6,6'-tetraphenyl-dipyranylidene and its use as a hole-collecting interfacial layer in organic solar cells

M. Courté,[‡a] M. Alaaeddine,[‡b,c,d] V. Barth,[b,c,d] L. Tortech,[b,c,d] and D. Fichou [a,b,c,*]

- Dipyranylidene acts as an efficient anodic interlayer in organic solar cells.
- It possesses excellent hole transporting/electron blocking properties.
- Photocurrent densities up to 11.5 mA/cm2 are recorded under AM 1.5G
- Conversion efficiencies up to 4.6% are attained, higher than PEDOT:PSS-only devices
- The origin is also to be found in the high crystallinity of dipyranylidene films.